Progress in Reaction Kinetics and Mechanism

ARTICLE

Open Access

https://doi.org/10.48130/prkm-0025-0003

Progress in Reaction Kinetics and Mechanism **2025**, 50: e003

Insights into the NO removal mechanism by hydrazine

Menglei Zheng and Xiaoyuan Zhang*

Department of Thermal Science and Energy Engineering, University of Science and Technology of China (USTC), Hefei 230026, Anhui, China

* Corresponding author, E-mail: xiaoyuanzhang@ustc.edu.cn

Abstract

Hydrazine (N_2H_4) can be a better reductant than ammonia (NH_3) for NO removal during the selective non-catalytic reduction (SNCR) process due to its wider temperature window. To better understand the $DeNO_x$ chemistry by N_2H_4, this study conducted a kinetic modeling study for $N_2H_4/NO/O_2$ based on recent NH_3 oxidation models. Compared with previous kinetic models, the present model is more accurate in predicting a four-stage NO removal phenomenon over 673−1,523 K. In Stage I (673−848 K), N_2H_4 is more favorable to produce NH_2 via N1 pathways, which mainly reacts with NO to proceed $DeNO_x$ pathways. In Stage II (848−1,048 K), the reaction sequence $N_2H_4 \rightarrow N_2H_3 \rightarrow H_2NN \rightarrow NO_2 \rightarrow NO$ prevails, decreasing NO_x removal ratios. In Stage III (1,048−1,248 K), the branching fraction of $H_2NN = N_2H_2$ increases, resulting in less NO_2 and more N_2H_2 being produced. The NO removal efficiency is further increased. When the temperature exceeds 1,248 K, i.e. Stage IV, NH_2 is favorable to produce NH via H-abstraction reactions, which can be subsequently oxidized to produce NO. Additionally, the present model is also validated against experimental data at various oxygen contents, suggesting that the NO removal efficiency is less affected by the oxygen concentration.

Citation: Zheng M, Zhang X. 2025. Insights into the NO removal mechanism by hydrazine. *Progress in Reaction Kinetics and Mechanism* 50: e003 https://doi.org/10.48130/prkm-0025-0003

Introduction

The combustion of fossil fuels is the main source of nitrogen oxide (NO_x) emissions[1,2], which have led to serious environmental problems. Recently, ammonia (NH_3) has been proposed and used to mitigate the impact of greenhouse gas (GHG) as a promising carbon-free fuel, which further exacerbates nitrogen oxide emissions[3]. To control NO_x pollution, selective catalytic reduction[4,5] (SCR) and selective non-catalytic reduction[6] (SNCR) stand out prominently for the treatment of flue gas after combustion. Both methods can convert NO_x to harmless N_2 through chemical reactions. Compared with SCR, SNCR does not require the use of expensive catalysts and therefore has a relatively low operation cost.

Since the SNCR of NO by NH_3 was proposed by Lyon in the 1970s[7], $DeNO_x$ chemistry has been intensively studied over a long period. NH_3 and urea have been widely used as reducing agents[8–10]. Extensive experimental and kinetic studies have confirmed that NO removal by NH_3 and urea relies mainly on the reactions of NH_2 + NO. However, the traditional SNCR has a relatively high and narrow temperature window (1,100−1,500 K), which limits its application at lower temperatures. Moreover, fluctuations in the oxygen concentration have significant adverse effects on the $DeNO_x$ efficiency and further elevate the temperature window[9].

Hydrazine (N_2H_4), another reducing agent, is widely used in rocket fuels, antioxidants, and pesticide materials[11,12]. Many studies have focused on the decomposition of N_2H_4[13–17], whereas few have reported NO removal by N_2H_4. In 1967, Sawyer & Glassman[18] first reported the gas-phase reactions of N_2H_4, NO_2, and NO in a flow tube under oxygen conditions. They proposed that the cleavage of the N-N bond is a prerequisite to react with NO, which confirmed the ability of N_2H_4 to remove NO. In 1985, Azuhata et al.[19] explored the applicability of N_2H_4 in NO_x removal and reported that N_2H_4 can remove NO in the temperature range of 773−873 K. Similarly, Lee & Kim[20] reported that the optimum reaction temperature for NO removal by N_2H_4 was 873 K, and the best normalized stoichiometric ratio (NSR) was 4.0. Based on the above studies, it is proven that N_2H_4 can lower the temperature window and could be a better reducing agent than ammonia.

However, unlike $DeNO_x$ studies of NH_3, kinetic modeling studies on the NO removal by N_2H_4 are insufficient, which hinders practical applications. Konnov & Ruyck[21] developed a kinetic model of N_2H_4 to describe its thermal decomposition and flame chemistry. They indicated that the initial decomposition reaction of N_2H_4 and the subsequent reaction of $NH_3 + NH_2$ had high sensitivities to the overall decomposition rate of N_2H_4 under highly diluted conditions. Later, Hong et al.[22] reported that N_2H_4 has a four-stage NO removal phenomenon and established a kinetic model to predict it. Moreover, their study revealed that the NO removal efficiency of N_2H_4 can bear an increase in oxygen concentration within a certain range. However, previous models[21,23] cannot accurately predict the NO removal efficiency, and a detailed explanation of $DeNO_x$ chemistry by N_2H_4 is also inadequate.

In this work, a kinetic model of $N_2H_4/NO/O_2$ is developed based on recent NH_3 models to predict the experimental data[23] of $N_2H_4/NO/O_2$ over 673−1,523 K. Through the kinetic modeling analysis, the four-stage NO removal phenomenon observed in the experiments is thoroughly explained, and the competitive relationship between the NO formation and $DeNO_x$ pathways is revealed. In addition, the effects of the oxygen content on NO removal by N_2H_4 are also discussed in detail.

Chemical kinetic model

This study reports a detailed kinetic model for the $N_2H_4/NO/O_2$ system, which is based on a recent NH_3/H_2 model from Zhu et al.[24]. Zhu et al. recently developed their model based on a widely used H_2/O_2 model from NUIGMech1.3[25], and the NH_2 related mechanisms, including pyrolysis, oxidation, and $DeNO_x$ reactions, were evaluated and thoroughly incorporated[26–28]. In addition, N_2H_4 and NO_x-related reactions were included in their model, which is based on the work of Glarborg et al.[29] and Sahu et al.[30], respectively. Their model is applicable for predicting the validation targets at 500−3,200 K and 0.08−75 atm. N_2H_4 can generate both N1 and N2

pathways. Specifically, the N1 pathway involves primarily NH_2 and NH radicals, whereas the N2 pathway includes a variety of N2 radicals (e.g. N_2H_3, N_2H_2, and H_2NN). The present model updated the rate constant of some critical reactions related to those radicals based on previous studies[21,31–35]. Important reactions discussed later are summarized in Table 1.

Important reactions related to the N2 pathway

The important reactions of the N2 pathway include the unimolecular decomposition reaction of N_2H_4 and bimolecular reactions, such as H-abstraction reactions of N_2H_4 and other N2 radicals. Among them, the rate constant of R1 has been investigated by several groups[16,17,21,29,36–39]. Konnov & Ruyck[21] estimated the rate constants of N_2H_4 decomposition from updated thermodynamic data and successfully predicted the experimental data of N_2H_4 decomposition. Therefore, the present model adopted the rate constant of R1 from theirs. The H-abstraction reaction of N_2H_4 by OH (R2) was adopted from the kinetic model of Chen et al.[35] to better predict the $DeNO_x$ process by N_2H_4. Gao et al.[40] measured the rate constant of R3 through laser photolysis/laser-induced fluorescence (LP-LIF) and computationally investigated the rate constant via quantum chemistry, which was adopted in this model. Additionally, the rate constants of H-abstraction reactions of N_2H_3 by different radicals (i.e. R4–R6) were adopted from Dean & Bozzelli[41] via direct hydrogen transfer (DHT) estimation. Meanwhile, the isomerization of H_2NN (R7) was also adopted from Dean & Bozzelli[41] via quantum Rice-Ramsperger-Kassel (QRRK) calculations. The decomposition reaction of H_2NN (R8) was adopted from Hwang & Mebel[34] via theoretical calculations. The rate constants for other reactions associated with H_2NN, N_2H_3, N_2H_2, and NNH were adopted from previous studies[10,32,42].

Table 1. Important reactions in the $N_2H_4/NO/O_2$ system. The parameters for use are in the modified Arrhenius expression $k = AT^{\beta}exp[-E/(RT)]$.

	Reactions	A ($cm^3 \cdot mol^{-1} \cdot s^{-1}$)	β (unitless)	Ea ($cal \cdot mol^{-1}$)	Ref.
R1	N_2H_4 (+ M) = $2NH_2$ (+ M)	5.0E14	0.000	251.22	[21]
	Low/	1.5E15	0.000	39000	
	N_2/ 2.4/ NH_3/ 3.0/ N_2H_4/ 4.0/				
R2	$N_2H_4 + OH = N_2H_3 + H_2O$	4.0E13	0.000	0.0000	[35]
R3	$N_2H_4 + NH_2 = N_2H_3 + NH_3$	3.8E01	3.440	−574.00	[40]
R4	$N_2H_3 + OH = H_2NN + H_2O$	3.0E13	0.000	0.0000	[41]
R5	$N_2H_3 + HO_2 = N_2H_2 + H_2O_2$	2.8E04	2.690	−1600.0	[41]
R6	$N_2H_3 + OH = N_2H_2 + H_2O$	1.2E06	2.000	−1192.0	[41]
R7	$N_2H_2 = H_2NN$	1.0 E01	0.000	0.0000	[41]
	PLOG / 1.0E-01	9.2E38	−9.010	67727/	
	PLOG / 1.0E+00	2.0E41	−9.380	68452/	
	PLOG / 1.0E+01	1.3E45	−1.013	70757/	
R8	$H_2NN = H_2 + N_2$	5.0E13	0.000	52785	[34]
R9	$NH_2 + NO = NNH + OH$	4.3E10	0.294	−866.00	[43]
R10	$NH_2 + NO = H_2O + N_2$	2.6E19	−2.369	870.00	[43]
R11	$NNH = N_2 + H$	3.0E08	0.000	0.0000	[41]
R12	$NNH + O_2 = N_2 + HO_2$	5.6E14	−0.385	−13.000	[44]
R13	$N_2H_2 + NO = N_2O + NH_2$	4.0E12	0.000	11922	[41]
R14	$N_2O + H = N_2 + OH$	6.7E10	0.000	5390.0	[45]
	Duplicate	4.4E14	0.000	18900	
R15	$NH_2 + NO_2 = H_2NO + NO$	1.1E12	0.110	−1186.0	[31–33]
	Duplicate	−4.3E17	−1.874	588.00	
R16	$H_2NO + NO_2 = HNO + HONO$	3.0E11	0.000	2000.0	[46]
R17	$H_2NO + O_2 = HNO + HO_2$	2.3E05	2.190	18000	[46]
R18	$HNO + O_2 = HO_2 + NO$	2.0E13	0.000	14000	[41]
R19	$H_2NN + O_2 = NH_2 + NO_2$	1.5E12	0.000	5961.0	[41]
R20	$NH_2 + OH = H_2O + NH$	3.3E06	1.949	−217.00	[47]
R21	$NH + O_2 = HNO + O$	3.3E09	1.034	11420	[3]
R22	$NH + O_2 = NO + OH$	4.5E08	0.790	1195.0	[48]

Important reactions related to the $DeNO_x$ process

The reactions of NH_2 and N_2H_2 with NO play crucial roles in NO removal by N_2H_4. Through R9 and R10, NH_2 converts NO to NNH and N_2, respectively, and NNH can further be converted to N_2[44] (i.e. R11 and R12), effectively leading to NO removal. Song et al.[43] measured the rate constants of R9 and R10 through shock tube experiments between 1,716 and 2,507 K, and fitted their measurements to cover 300–2,500 K based on previous results at lower temperatures. The final fitted results were adopted in this model to predict the experimental data under wide temperature conditions. Unlike NH_3, N_2H_4 proceeds through N2 pathways to produce N_2H_2, which combines with NO to produce N_2O. R13 was adopted from the evaluated results of Dean & Bozzelli[41]. N_2O then reacts with H to ultimately produce harmless N_2[31] (i.e. R14). The above reactions constitute the $DeNO_x$ mechanism in the present model.

Important reactions related to the NO_x formation process

NH_2 consumes NO_2 via the chain-propagation reaction R15 and simultaneously generates NO and H_2NO, which can further be converted to NO via H-loss reactions (i.e. R16–R18). Glarborg[32] re-evaluated the rate constant of this reaction, which aligns with the theoretical calculation results of Klippenstein et al.[33], and hence was adopted in this model. Stagni & Cavallotti[46] investigated a series of H-abstraction reactions from H_2NO (i.e. R16 and R17) via CASPT2 calculations and their calculated results were adopted in this model. The reaction between H_2NN and oxygen to form NO_2 (i.e. R19) was referred to the comprehensive review by Dean & Bozzelli[41]. The rate constant of R20 was adopted from theoretical calculation results from Klippenstein et al.[47], which are consistent with experimental measurements[47,49]. In addition, the NO_x formation pathways also involve the oxidation of NH under high-temperature conditions (i.e. R21 and R22). The rate constant of R21 was adopted from the evaluated value from Elishav et al.[3].

Simulation method

In this study, the perfect stirred reactor (PSR) module in ANSYS CHEMKIN-PRO[50] software was used for the simulations. The simulation conditions are consistent with those of Guan et al.[23]. The detailed simulation conditions are summarized in Table 2. Since NO_x mainly comes from the combustion of hydrocarbon fuels, which simultaneously produces H_2O and CO_2 as major products. CO_2 and H_2O, accompanied with NO_x were adopted to stimulate flue gas components. The complete kinetic mechanism comprises 43 species and 313 reactions, and the kinetic, thermodynamic, and transport files of this model can be found in the supplementary information.

Table 2. Validation conditions[23] of the present model.

Parameters	Condition 1	Condition 2	Condition 3
T (K)	673–1,523	773–1,398	773–1,348
P (atm)	1	1	1
τ (s)	0.3	0.3	0.3
NO (ppm)	450	500	500
N_2H_4 (ppm)	450	1,000	1,000
NSR	2	4	4
O_2 (%)	18–4.74	7.4–16.5	9.9–16.8
CO_2 (%)	5	5	5
H_2O (%)	10	10	10
N_2 (%)	Balance	Balance	Balance

Results and discussion

Model validation

To better interpret the NO removal efficiency by N_2H_4, the simulated mole fractions of NO are converted to the NO removal ratios (η). It is calculated via Eq. (1), where NO_{inlet} and NO_{outlet} represent the NO inlet and outlet concentration, respectively. Figure 1 shows the comparison between the measured and predicted NO removal ratios of the present model, as well as those of previous models[23,24,32,51,52]. Among previous models, three of them[23,24,32] include recent kinetic models of NH_3 oxidation and $DeNO_x$ chemistry by NH_3 or N_2H_4. Guan et al.[23] conducted experimental and simulation results for NO removal by N_2H_4. Chen et al.[51] developed a kinetic model to predict the laminar burning velocities of $NH_3/O_2/Ar$. Glarborg[32] updated critical reactions in NH_3 ignition and N_2O formation and presented a model for the $NH_3/NO_2/O_2$ system. Thomas et al.[52] developed an NH_3 model to predict the extinction of NH_3/H_2 flames and the formation of NO. Zhu et al.[24] developed a comprehensive NH_3/H_2 kinetic model over a wide range of temperatures and pressures. These literature models are named as Guan 2019, Konnov 2023, Glarborg 2023, Shrestha 2023, and Zhu 2024, respectively. The experiment results of Guan 2019 and the simulation results of the present model show that NO removal by N_2H_4 is dependent on temperature, resulting in a four-stage NO removal phenomenon.

$$\eta = \frac{NO_{inlet} - NO_{outlet}}{NO_{inlet}} \quad (1)$$

Compared with other models, the model proposed in this study demonstrates greater accuracy in capturing this non-monotonous trend, as shown in Fig. 1. Specifically, recently published kinetic models related to ammonia oxidation, such as Konnov 2023[51], Glarborg 2023[32], Shrestha 2023[52], and Zhu 2024[24], show different trends from experimental data. In the temperature range of 800–973 K, the Konnov 2023 model predicts negative NO removal ratios, which is the opposite of experimental observations. To better present and compare the NO removal efficiency of different models, the NO removal ratios below −15% are not shown in Fig. 1. Compared with the Guan 2019 model[23], the present model performs better in predicting the peak NO removal efficiency. Additionally, simulations are conducted to predict the experimental data with different oxygen concentrations, as shown in Figs 2 and 3. The results indicate that compared with previous models[24,32,51,52], the present model can better predict the four-stage NO removal behavior, although it still needs to be improved over 1,100–1,300 K. Therefore, recent comprehensive kinetic models for NH_3 oxidation are not applicable in the investigation of NO removal by N_2H_4, since the N_2H_4 sub-mechanism and its interaction with NO have not been well tested. The uncertainties of the present model may come from both the kinetic parameters and simulation methods. The rate constants of N2-related reactions are mainly from estimations. Future efforts involving experiments and theoretical calculations are highly needed. In addition, the simulations are based on the PSR module, while the experimental process[23] makes it difficult to achieve the complete mixing state. Therefore, the perfect-stirred assumption may introduce extra uncertainties to the simulation results. Future work on improving the simulation methods is required.

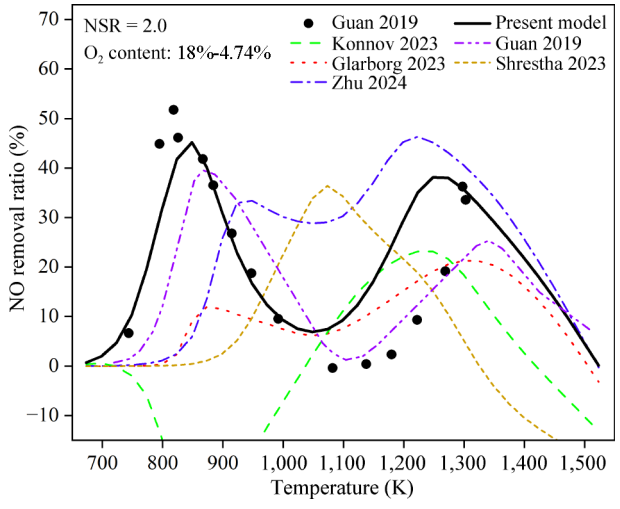

Fig. 1 NO removal ratios of $N_2H_4/NO/O_2$ under condition 1. The symbols are experimental data from previous work[23]. The solid, dash dot dotted, dashed, dotted, short dashed, and dash dotted lines are the predicted results by the present, Guan 2019[23], Konnov 2023[51], Glarborg 2023[32], Shrestha 2023[52] and Zhu 2024[24] models, respectively.

Reaction kinetics of the four-stage NO removal behavior

The NO removal efficiency is the result of the competition between NO formation and $DeNO_x$ pathways[53]. To elucidate the

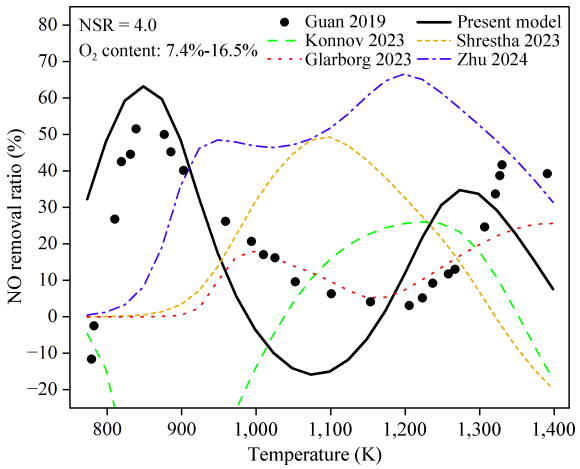

Fig. 2 NO removal ratios of $N_2H_4/NO/O_2$ under condition 2. The symbols are experimental data from previous work[23]. The solid, dashed, dotted, short dashed, and dash dotted lines are the predicted results of the present, Konnov 2023[51], Glarborg 2023[32], Shrestha 2023[52], and Zhu 2024[24] models, respectively.

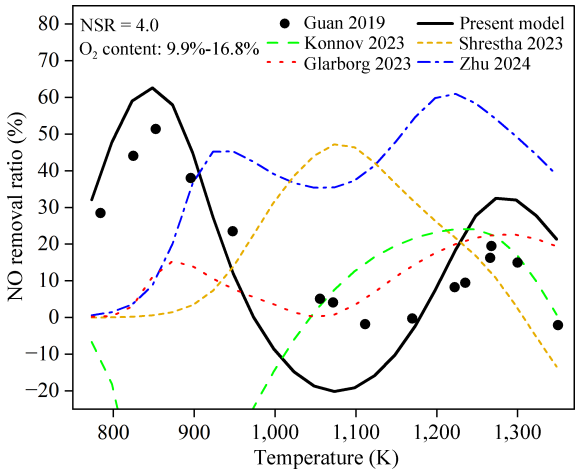

Fig. 3 NO removal ratios of $N_2H_4/NO/O_2$ at condition 3. The symbols are experimental data from previous work[23]. The solid, dashed, dotted, short dashed, and dash dotted lines are the predicted results of the present, Konnov 2023[51], Glarborg 2023[32], Shrestha 2023[52], and Zhu 2024[24] models, respectively.

mechanism of NO removal by N_2H_4, rate of production (ROP) analyses were conducted in this work. As shown in Fig. 4a, N_2H_4 proceeds via both the N1 and N2 pathways to generate NH_2 and N_2H_3 (yellow box), respectively. These two radicals further participate in both the $DeNO_x$ (green box) and NO formation (red box) pathways. The dashed arrows represent the pathways that are important only under high-temperature conditions. The mole fractions of critical species related to the $DeNO_x$ and NO formation pathways are shown in Fig. 4b & c. Both the experimental and simulation results of the present model reveal that NO removal exhibits a four-stage process. Based on the model analyses, the NO removal mechanism of each stage is analyzed in this section. Detailed reaction pathways of N_2H_4 at four typical temperatures corresponding to each stage are presented in Supplementary Figs S1–S4.

NO removal mechanism in Stage I

Stage I (i.e. 673–848 K) can be considered as a $DeNO_x$ region, since the mole fraction of NO decreases. In this stage, more than 75% of the N_2H_4 is consumed, while N_2H_2 and NH_2 radicals reach their first peak values, as shown in Fig. 4b. To study the NO removal chemistry of this stage, ROP analyses were conducted at 798 K. The results reveal that N_2H_4 is consumed mainly through the unimolecular decomposition reaction R1 to produce NH_2, as well as H-abstraction reactions by OH (i.e. R2) and NH_2 (i.e. R3) to generate N_2H_3. In this stage, the NH_2 radical mainly reacts with NO to produce NNH and N_2 via R9 and R10, respectively. While its reaction with NO_2 to produce NO via R15 is not competitive, since the mole fraction of NO_2 in this stage is very low, as seen in Fig. 4c. Therefore, the NH_2-related pathway mainly results in the $DeNO_x$-process, which can be confirmed by the sensitivity analysis results shown in Fig. 5. In contrast, N_2H_3 produced via R4 and R5 can be consumed by OH and HO_2 to produce H_2NN and N_2H_2, respectively. Both pathways are important in Stage I. N_2H_2 mainly reacts with NO to proceed the $DeNO_x$ pathways via R13, while H_2NN is almost completely converted to NO_2 via R19 in this stage. Therefore, the N_2H_3-related pathway contributes to both the $DeNO_x$ and NO_x formation process. Combining the NH_2 and N_2H_3 related pathways, the $DeNO_x$ pathway are more favorable than the NO_x formation pathway in Stage I, leading to the increase of NO removal ratios, as seen in Fig. 1. In addition, since most of the NH_2 radicals from N_2H_4 decomposition contribute to the $DeNO_x$ process, while only half of the fuel radicals N_2H_3 proceed $DeNO_x$ pathways via N_2H_2, as seen from Supplementary Fig. S1. $DeNO_x$ reactions related to NH_2 (R9 and R10) present larger negative sensitivity coefficients than those of N_2H_2 (R13) for NO formation in this stage, as seen in Fig. 5. This finding indicates that the N1 pathways via NH_2 are more effective than the N2 pathways in Stage I.

NO removal mechanism in Stage II

As the temperature increases to Stage II (i.e. 848–1,048 K), the mole fraction of N_2H_2 starts to decrease, while those of H_2NN and NO_2 greatly increase (see Fig. 4c). The NO removal ratios decrease in this stage, as seen in Fig. 1. Compared with Stage I, significant changes in the reaction pathways of NH_2 and N_2H_3 radicals occur in this stage. For the NH_2 pathways, the branching fraction of R15 ($NH_2 + NO_2 = H_2NO + NO$) increases, promoting the formation of NO. Meanwhile, H_2NO can be converted into NO through a series of H-loss reactions (i.e. R16–R18). Therefore, R15 has a strongly positive sensitivity coefficient for NO formation in this stage, indicating that this reaction plays a key role in NO_x formation, as shown in Fig. 5. For the N_2H_3 pathways, it is more inclined to generate H_2NN via R4 rather than N_2H_2 via R5. As mentioned above, N_2H_2 and H_2NN are two functionally distinct radicals. The former tends to participate in the $DeNO_x$ process, while the latter is more inclined to react with oxygen and generate NO_x. Therefore, the reaction produces H_2NN via R4 exhibits positive sensitivity coefficients for NO formation, as seen from Fig. 5. It is surprising that R9 ($NH_2 + NO = NNH + OH$) presents positive sensitivity coefficient for NO formation in this stage. This is because this reaction produces OH radical, which is critical for converting N_2H_3 to H_2NN via R4 ($N_2H_3 + OH = H_2NN +$

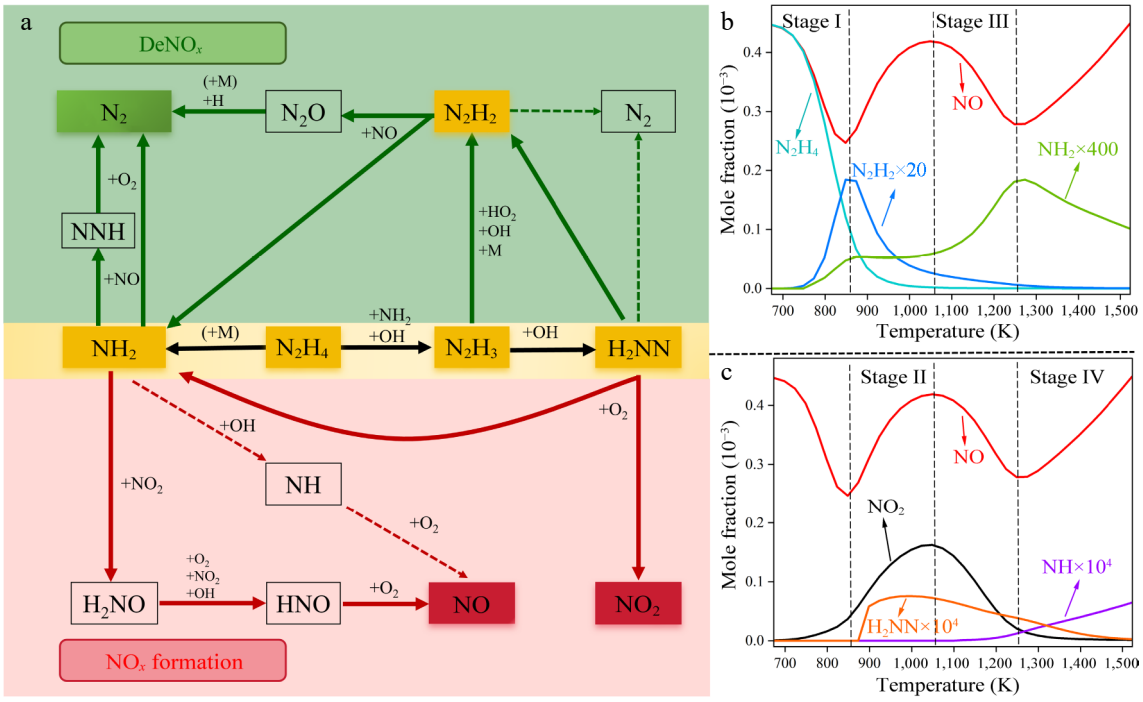

Fig. 4 (a) Reaction pathways of N_2H_4 under condition 1. The green and red boxes highlight reaction pathways involved in the $DeNO_x$ and NO_x formation processes, respectively. The dashed arrows represent the pathways that are important only under high-temperature conditions. (b), (c) Simulated mole fractions of critical species in the $N_2H_4/NO/O_2$ under condition 1.

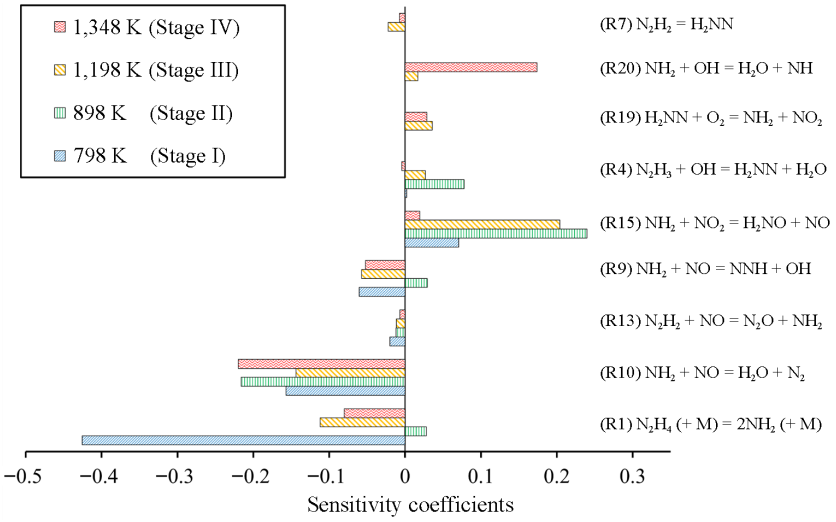

Fig. 5 Sensitivity analysis of NO at 798, 898, 1,198, and 1,348 K, corresponding to Stage I to IV, under condition 1.

H_2O). Since the flux of R4 increases significantly, the mole fraction of H_2NN dramatically increases, which simultaneously promotes the formation of NO_2 in this stage via R19 ($H_2NN + O_2 = NH_2 + NO_2$), as shown in Fig. 4c. In summary, in this stage, the reaction sequence $N_2H_4 \rightarrow N_2H_3 \rightarrow H_2NN \rightarrow NO_2 \rightarrow NO$ and R15 prevail, leading to an increase in the NO_x concentration.

NO removal mechanism in Stage III

In Stage III (i.e. 1,048–1,248 K), N_2H_4 is completely consumed, and an obvious downward trend in the NO content can be observed again. Besides, the mole fractions of H_2NN and NO_2 present decreasing trends, while that of NH_2 starts to increase again as shown in Fig. 4b & c. In Stage II, H_2NN is completely converted to NO_2 via R19. However, in Stage III, the branching fraction of $H_2NN = N_2H_2$ increases, as shown in Fig. 4a. This change leads to less NO_2 formation (see Fig. 4c), and further reduces NO formation via R15 ($NH_2 + NO_2 = H_2NO + NO$). Therefore, the flux of $H_2NN \rightarrow NO_2 \rightarrow NO$ decreases. Meanwhile, the content of NH_2 increases so that the $DeNO_x$ process via R9 and R10 becomes favorable. Therefore, R1 as the main source of NH_2, shows negative sensitivity coefficient again compared with Stage II, as shown in Fig. 5. On the other hand, this reaction successfully converts H_2NN to N_2H_2, which can effectively promote NO removal via R13 ($N_2H_2 + NO = N_2O + NH_2$). The sensitivity analysis further demonstrates that R7 ($N_2H_2 = H_2NN$) has a negative sensitivity coefficient for NO formation and thus promotes NO removal. Therefore, the $DeNO_x$ pathway plays a dominant role again.

NO removal mechanism in Stage IV

In Stage IV (i.e. 1,248–1,523 K), the NH_2 radical tends to consume, while the NH radical greatly increases, as shown in Fig. 4b & c. Under these high-temperature conditions, NH_2 prefers to combine with OH to produce NH, which further reacts with O_2 to generate NO via R20–R22. Therefore, R20 ($NH_2 + OH = H_2O + NH$) has a strongly positive sensitivity coefficient for NO formation, as shown in Fig. 5. For N2 species shown in Fig. 4c, H_2NN remains and continues to be consumed. Compared with Stage III, the H_2NN tends to produce N_2 via the unimolecular decomposition reaction R8 ($H_2NN = N_2 + H_2$), as shown in Fig. 4a (the dashed lines). Other pathways of H_2NN, such as the formation of N_2H_2 and NO_2, are less important, indicating that the N2 pathways in this stage have little influence on NO formation. Therefore, in this stage, NO formation is favorable due to the reaction sequence of $NH_2 \rightarrow NH \rightarrow NO$.

Above all, compared with NH_3, N_2H_4 can achieve SNCR of NO over wider temperature windows. The chain-initiation reaction of NH_3 occurs at high temperatures (above 1,100 K) due to the strong N-H bond dissociation energy. However, much weaker N-N and N-H bonds in N_2H_4 make chain-initiation reactions of N_2H_4 easier to occur, resulting in a much lower $DeNO_x$ temperature window (i.e. 673–848 K). In addition, the special N2 pathways in N_2H_4 have two opposite effects: the production of N_2H_2 promotes the $DeNO_x$ process via R13, which is not found important in the NH_3 $DeNO_x$ system; and the production of H_2NN inhibits the $DeNO_x$ process due to the formation of NO_2 via R19. The enhanced formation of NO_2 further promotes NO formation via R15 ($NH_2 + NO_2 = H_2NO + NO$).

Effects of the oxygen content on NO removal

The increased oxygen content enhances the oxidation reactions by increasing the mole fractions of oxygenated species such as O_2, OH, and HO_2. These radicals play important roles in the removal and formation process of NO[54]. The effects of the oxygen content on NO removal by N_2H_4 are simulated by the present model, and the results are compared in Fig. 6.

Both the experimental and simulation results suggest that the NO removal ratio is not strongly affected by the oxygen content. However, at approximately 1,350 K, the experimental results show

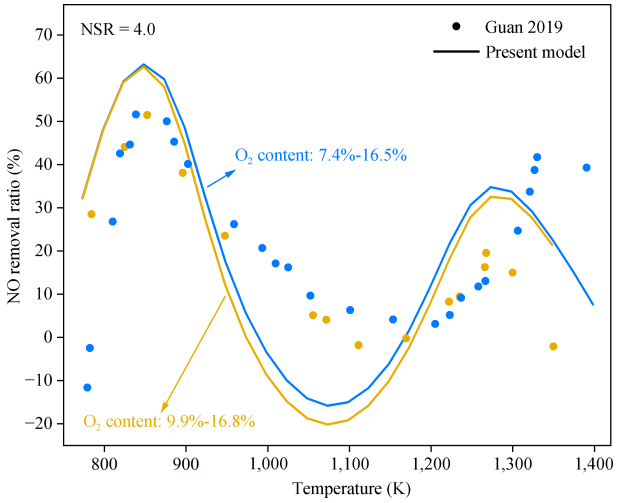

Fig. 6 Effect of O_2 content on the removal of NO at $[NO]_{initial}$ = 500 ppm, NSR = 4.0 at 1 atm and τ = 0.3 s. Symbols are experimental data from Guan 2019[23], while lines are the predicted results by the present model.

that an increase in the oxygen content leads to a significant decrease in the NO removal ratio, while the simulation results indicate that this effect is minimal. This could be attributed to the experimental uncertainties since only one point presents a large discrepancy. Based on model analyses, N_2H_4 initially generates NH_2 radical via its unimolecular decomposition reaction R1 without oxidative pathways, while in the NH_3 DeNO$_x$ system, NH_2 is generated mainly via H-abstraction reactions by OH, O, and HO_2 radicals[55]. Since NH_2 is the main radical for NO removal in both systems, the N_2H_4 system is less influenced by the oxygen content. Nevertheless, the formation of N_2H_2 is related to oxygenated radicals such as OH and HO_2, so the influence of oxygen content still exists. Above all, compared with NH_3, it is testified that N_2H_4 has a wider range of oxygen fractions for NO removal during the SNCR process. Therefore, another advantage of using N_2H_4 for the SNCR of NO is that its NO removal efficiency is relatively less affected by fluctuations in the oxygen content. This characteristic enables N_2H_4 to play a more stable role in the SNCR process, which fits better with the practical flue gas treatment environment after combustion.

Conclusions

In this work, a kinetic model for NO removal by N_2H_4 was developed. The simulation results of this model were reasonably consistent with the experimental data over the temperature range of 673−1,523 K. Compared with recently published kinetic models, the present model was more accurate in predicting the temperature window and peak values of the NO removal efficiency. It has also been demonstrated that recent NH_3 oxidation models are not accurate enough for predicting NO removal by N_2H_4, although they have been comprehensively validated against wide experimental targets of NH_3. Both the experimental and simulation results of this model present a four-stage NO removal trend by N_2H_4.

Based on the model analysis, it revealed that N_2H_4 can generate N1 and N2 pathways to achieve DeNO$_x$ and the NO formation process. In the N1 pathway, NH_2 can undergo the reactions of DeNO$_x$ and NO formation simultaneously. In the N2 pathway, N_2H_3 produces N_2H_2 and H_2NN. N_2H_2 tends to participate in the DeNO$_x$ process, while H_2NN tends to react with O_2 to generate NO$_x$. In Stage I (673−848 K), N_2H_4 generates NH_2 and N_2H_2 through N1 and N2 pathways, respectively, both of which can promote NO removal via R9, R10, and R13, with N1 pathway being more effective. Since the chain-initiation reactions in the N_2H_4 DeNO$_x$ system have lower energy barriers than that in NH_3, the DeNO$_x$ process by N_2H_4 occurs at lower temperatures. In Stage II (848−1,048 K), the reaction sequence $N_2H_4 \rightarrow N_2H_3 \rightarrow H_2NN \rightarrow NO_2 \rightarrow NO$ and R15 ($NH_2 + NO_2 = H_2NO + NO$) prevailed, increasing the content of NO$_x$ and decreasing the efficiency of NO removal by N_2H_4. When the temperature increased to Stage III (1,048-1,248 K), the flux of $H_2NN = N_2H_2$ increased, leading to less NO_2 and more N_2H_2 being produced, increasing NO$_x$ removal efficiency again. When the temperature exceeds 1,248 K, i.e. Stage IV, NH_2 prefers to produce NH via H-abstraction reactions, and NH further reacts with O_2 to generate NO. Furthermore, the simulation results suggested that NO removal by N_2H_4 is less affected by the fluctuations of oxygen content. The main reason is that N_2H_4 can be converted to NH_2 directly via the unimolecular decomposition reaction R1, whereas in the NH_3 DeNO$_x$ system, NH_2 is generated mainly via H-abstraction reactions by OH, O and OH_2. These findings are highly important for better understanding the chemistry of NO removal by N_2H_4.

Author contributions

The authors confirm contribution to the paper as follows: study conception and design: Zheng M, Zhang X; data collection: Zheng M; analysis and interpretation of results: Zheng M, Zhang X; draft manuscript preparation: Zheng M, Zhang X. Both authors reviewed the results and approved the final version of the manuscript.

Data availability

All data generated or analyzed during this study are included in this published article and its supplementary information files.

Acknowledgments

The authors are grateful for the funding support from the National Natural Science Foundation of China (22403085) and the Natural Science Foundation of Anhui Province (2408085MB034).

Conflict of interest

The authors declare that they have no conflict of interest.

Supplementary information accompanies this paper at (https://www.maxapress.com/article/doi/10.48130/prkm-0025-0003)

Dates

Received 7 November 2024; Revised 3 December 2024; Accepted 15 January 2025; Published online 13 February 2025

References

1. Yuan B, Mao X, Wang Z, Hao R, Zhao Y. 2020. Radical-induced oxidation removal of multi-air-pollutant: A critical review. *Journal of Hazardous Materials* 383:121162
2. Lin F, Wang Z, Zhang Z, He Y, Zhu Y, et al. 2020. Flue gas treatment with ozone oxidation: An overview on NO_x, organic pollutants, and mercury. *Chemical Engineering Journal* 382:123030
3. Elishav O, Mosevitzky Lis B, Miller EM, Arent DJ, Valera-Medina A, et al. 2020. Progress and prospective of nitrogen-based alternative fuels. *Chemical Reviews* 120:5352−436
4. Shan W, Yu Y, Zhang Y, He G, Peng Y, et al. 2021. Theory and practice of metal oxide catalyst design for the selective catalytic reduction of NO_x with NH_3. *Catalysis Today* 376:292−301
5. Sun Y, Zwolińska E, Chmielewski AG. 2016. Abatement technologies for high concentrations of NO_x and SO_2 removal from exhaust gases: A review. *Critical Reviews in Environmental Science and Technology* 46:119−42
6. Tayyeb Javed M, Irfan N, Gibbs BM. 2007. Control of combustion-generated nitrogen oxides by selective non-catalytic reduction. *Journal of Environmental Management* 83:251−89
7. Lyon RK. 1976. The NH_3-NO-O_2 reaction. *International Journal of Chemical Kinetics* 8:315−18
8. Mahmoudi S, Baeyens J, Seville JPK. 2010. NO_x formation and selective non-catalytic reduction (SNCR) in a fluidized bed combustor of biomass. *Biomass and Bioenergy* 34:1393−409
9. Rahman ZU, Wang X, Zhang J, Baleta J, Vujanović M, et al. 2021. Kinetic study and optimization on SNCR process in pressurized oxy-combustion. *Journal of the Energy Institute* 94:263−71
10. Miller JA, Bowman CT. 1989. Mechanism and modeling of nitrogen chemistry in combustion. *Progress in Energy and Combustion Science* 15:287−338
11. Cobos CJ, Glarborg P, Marshall P, Troe J. 2023. Re-evaluation of rate constants for the reaction N_2H_4 (+ M) ⇄ $NH_2 + NH_2$ (+ M). *Combustion and Flame* 257:112374
12. Wu J, Bruce FNO, Bai X, Ren X, Li Y. 2023. Insights into the reaction kinetics of hydrazine-based fuels: a comprehensive review of theoretical and experimental methods. *Energies* 16:6006
13. Mchale ET, Knox BE, Palmer HB. 1965. Determination of the decomposition kinetics of hydrazine using a single-pulse shock tube. *Symposium (International) on Combustion* 10:341−51

14. Diesen RW. 1963. Mass spectral studies of kinetics behind shock waves. II. Thermal decomposition of hydrazine. *Journal of Chemical Physics* 39:2121–28
15. Moberly WH. 1962. Shock tube study of hydrazine decomposition. *The Journal of Physical ChemistryProgress in Energy and Combustion Science* 66:366–68
16. Szwarc M. 1949. The dissociation energy of the N-N bond in hydrazine. *Proceedings of the Royal Society of London. Series A: Mathematical and Physical Sciences* 198:267–84
17. Michel KW. 1965. Thermal decomposition of hydrazine. *Angewandte Chemie* 4(4):369–69
18. Sawyer RF, Glassman I. 1967. Gas-phase reactions of hydrazine with nitrogen dioxide, nitric oxide, and oxygen. *Symposium (International) on Combustion* 11:861–69
19. Azuhata S, Akimoto H, Hishinuma Y. 1985. The behavior of nitrogen-oxides in the N_2H_4-NO-O_2 reaction. *AIChE Journal* 31:1223–25
20. Lee JB, Kim SD. 1998. NO_x reduction by hydrazine in a pilot-scale reactor. *Chemical Engineering Journal* 69:99–104
21. Konnov AA, De Ruyck J. 2001. Kinetic modeling of the decomposition and flames of hydrazine. *Combustion and Flame* 124:106–26
22. Hong L, Chen D, Wang D, Huang S. 2012. Kinetic mechanism and characteristics researches for hydrazine-based NO_x removal at moderate to high temperatures. *Environmental Science* 33:2901–8
23. Guan Z, Hong L, Guo R, Pan W, Li F, et al. 2019. Improved NO removal from flue gas by hydrazine and its mechanism analysis. *Journal of Chemical Technology & Biotechnology* 94:3263–68
24. Zhu Y, Curran HJ, Girhe S, Murakami Y, Pitsch H, et al. 2024. The combustion chemistry of ammonia and ammonia/hydrogen mixtures: A comprehensive chemical kinetic modeling study. *Combustion and Flame* 260:113239
25. Panigrahy S, Mohamed AAE, Wang P, Bourque G, Curran HJ. 2023. When hydrogen is slower than methane to ignite. *Proceedings of the Combustion Institute* 39:253–63
26. Stagni A, Cavallotti C, Arunthanayothin S, Song Y, Herbinet O, et al. 2020. An experimental, theoretical and kinetic-modeling study of the gas-phase oxidation of ammonia. *Reaction Chemistry & Engineering* 5:696–711
27. Xu S, Lin MC. 2009. Ab initio chemical kinetics for the NH_2+HNO_x reactions, part III: Kinetics and mechanism for NH_2+$HONO_2$. *International Journal of Chemical Kinetics* 42:69–78
28. Klippenstein SJ, Glarborg P. 2022. Theoretical kinetics predictions for NH_2+HO_2. *Combustion and Flame* 236:111787
29. Glarborg P, Hashemi H, Cheskis S, Jasper AW. 2021. On the rate constant for NH_2+HO_2 and third-body collision efficiencies for NH_2+H(+M) and NH_2+NH_2(+M). *The Journal of Physical Chemistry A* 125:1505–16
30. Sahu AB, Mohamed AAE, Panigrahy S, Saggese C, Patel V, et al. 2022. An experimental and kinetic modeling study of NO_x sensitization on methane autoignition and oxidation. *Combustion and Flame* 238:111746
31. Glarborg P, Miller JA, Ruscic B, Klippenstein SJ. 2018. Modeling nitrogen chemistry in combustion. *Progress in Energy and Combustion Science* 67:31–68
32. Glarborg P. 2023. The NH_3/NO_2/O_2 system: constraining key steps in ammonia ignition and N_2O formation. *Combustion and Flame* 257:112311
33. Klippenstein SJ, Harding LB, Glarborg P, Gao Y, Hu H, et al. 2013. Rate constant and branching fraction for the NH_2 + NO_2 reaction. *The Journal of Physical Chemistry A* 117:9011–22
34. Hwang DY, Mebel AM. 2003. Reaction mechanism of N_2/H_2 conversion to NH_3: a theoretical study. *The Journal of Physical Chemistry A* 107:2865–74
35. Chen H, Chen D, Fan S, Hong L, Wang D. 2016. SNCR De-NO_x within a moderate temperature range using urea-spiked hydrazine hydrate as reductant. *Chemosphere* 161:208–18
36. Bahng MK, Macdonald RG. 2009. Determination of the rate constants for the radical-radical reactions $NH_2(X^{-2}B_1)$ + $NH(X^3\Sigma^-)$ and $NH_2(X^{-2}B_1)$ + $H(^2S)$ at 293 K. *The Journal of Physical Chemistry A* 113:2415–23
37. Patrick R, Golden DM. 1984. Kinetics of the reactions of amidogen radicals with ozone and molecular oxygen. *The Journal of Physical Chemistry* 88:491–95
38. Altinay G, Macdonald RG. 2015. Determination of the rate constants for the $NH_2(X^2B_1)$ + $NH_2(X^2B_1)$ and $NH_2(X^2B_1)$ + H recombination reactions in N_2 as a function of temperature and pressure. *The Journal of Physical Chemistry A* 119:7593–610
39. Gordon S, Mulac W, Nangia P. 1971. Pulse radiolysis of ammonia gas. II. rate of disappearance of the $NH_2(X^2B_1)$ radical. *The Journal of Physical Chemistry* 75:2087–93
40. Gao Y, Alecu IM, Hashemi H, Glarborg P, Marshall P. 2023. Reactions of hydrazine with the amidogen radical and atomic hydrogen. *Proceedings of the Combustion Institute* 39:571–79
41. Dean AM, Bozzelli JW. 2000. Combustion chemistry of nitrogen. In *Gas-phase combustion chemistry*, ed. Gardiner WC. New York, USA: Springer. pp. 125–341. doi: 10.1007/978-1-4612-1310-9_2
42. Diévart P, Catoire L. 2020. Contributions of experimental data obtained in concentrated mixtures to kinetic studies: application to monomethylhydrazine pyrolysis. *The Journal of Physical Chemistry A* 124:6214–36
43. Song S, Hanson RK, Bowman CT, Golden DM. 2001. Shock tube determination of the overall rate of NH_2 + NO → products in the thermal De-NO_x temperature window. *International Journal of Chemical Kinetics* 33:715–21
44. Klippenstein SJ, Harding LB, Glarborg P, Miller JA. 2011. The role of NNH in NO formation and control. *Combustion and Flame* 158:774–89
45. Marshall P, Ko T, Fontijn A. 1989. High-temperature photochemistry kinetics studies of the reactions of hydrogen atom(1^2S) and deuterium atom(1^2S) with nitrous oxide. *The Journal of Physical Chemistry* 93:1922–27
46. Stagni A, Cavallotti C. 2023. H-abstractions by O_2, NO_2, NH_2, and HO_2 from H_2NO: theoretical study and implications for ammonia low-temperature kinetics. *Proceedings of the Combustion Institute* 39:633–41
47. Klippenstein SJ, Harding LB, Ruscic B, Sivaramakrishnan R, Srinivasan NK, et al. 2009. Thermal decomposition of NH_2OH and subsequent reactions: Ab initio transition state theory and reflected shock tube experiments. *The Journal of Physical Chemistry A* 113:10241–59
48. Römming HJ, Wagner HG. 1996. A kinetic study of the reactions of $NH(X^3\Sigma^-)$ with O_2 and NO in the temperature range from 1200 to 2200 K. *Symposium (International) on Combustion* 26:559–66
49. Mousavipour SH, Pirhadi F, HabibAgahi A. 2009. A theoretical investigation on the kinetics and mechanism of the reaction of amidogen with hydroxyl radical. *The Journal of Physical Chemistry A* 113:12961–71
50. ANSYS. 2023. ANSYS Chemkin-Pro: a chemical kinetics package for analysis of gas-phase chemical kinetics. www.ansys.com/zh-cn/products/fluids/ansys-chemkin-pro
51. Chen J, Lubrano Lavadera M, Konnov AA. 2023. An experimental and modeling study on the laminar burning velocities of ammonia + oxygen + argon mixtures. *Combustion and Flame* 255:112930
52. Thomas DE, Shrestha KP, Mauss F, Northrop WF. 2023. Extinction and NO formation of ammonia-hydrogen and air non-premixed counterflow flames. *Proceedings of the Combustion Institute* 39:1803–12
53. Zhang X, Moosakutty SP, Rajan RP, Younes M, Sarathy SM. 2021. Combustion chemistry of ammonia/hydrogen mixtures: Jet-stirred reactor measurements and comprehensive kinetic modeling. *Combustion and Flame* 234:111653
54. Mei B, Zhang X, Ma S, Cui M, Guo H, et al. 2019. Experimental and kinetic modeling investigation on the laminar flame propagation of ammonia under oxygen enrichment and elevated pressure conditions. *Combustion and Flame* 210:236–46
55. Sabia P, Manna MV, Cavaliere A, Ragucci R, de Joannon M. 2020. Ammonia oxidation features in a jet stirred flow reactor. The role of NH_2 chemistry. *Fuel* 276:118054